Inter-satellite Optical Analog Network Coding Using Modulated Retro Reflectors

Jia Yanmei[1,2], Lyu Congmin[1,2], Shen Pengfei[1,2], and Lu Lu[1,2(✉)]

[1] University of Chinese Academy of Sciences, Beijing 100049, China
lulu@csu.ac.cn
[2] Technology and Engineering Center for Space Utilization, Chinese Academy of Sciences, Beijing 100094, China

Abstract. Information sharing, real-time data exchange, and low SWaP (Size, Weight and Power) inter-satellite communication are the key technologies for cooperative satellite. In order to build a high-throughput inter-satellite optical communication network suitable for micro-satellites, an analog network coding (ANC) system based on modulated retro reflectors (MRR) was designed for two way relay channel (TWRC). Different from traditional-scheduling (TS) based TWRC, MRR ANC saves two sets of pointing, acquisition and tracking (PAT) devices at the end terminals. Specifically, our proposed MRR ANC system is suitable for small satellites with tight SWaP constrains. In this paper, we solve the power allocation problem of MRR ANC using Lagrange multiplier method under sum rate maximization criteria. We evaluated the system throughput and bit error rate (BER) performances using numerical simulations. The results show that both sum rate and BER performances of MRR ANC are improved using our proposed method compared with conventional uniform power allocation scheme. When each bidirectional link distance is 200 km, the non-channel-coded BER of each terminal is 10^{-5} using on-off keying (OOK) modulation. Compared with traditional scheduling, the system throughput of MRR ANC was improved by 1.8 times.

Keywords: Modulated retro reflector · Analog network coding · Power allocation · Throughput

1 Introduction

With the development of space technology, the amount of information exchange and the data transmission rate between applied satellite systems is increasing. The demand for inter-satellite network is increasingly urgent. Small satellites have the characteristics of low cost, dynamic and flexible reconstruction, so it

This work was supported in part by the Key Research Program of the Chinese Academy of Sciences, under Grant ZDRW-KT-2019-1-0103.

S. Paiva et al. (Eds.): SmartCity360° 2021, LNICST 442, pp. 15–26, 2022.
https://doi.org/10.1007/978-3-031-06371-8_2

has become a trend to use small satellites to form a space-based integrated information network, information fusion and interconnection. Compared with radio frequency (RF) systems, free space optical communication (FSOC) has lower size, weight, and power (SWaP) advantages in addition to higher data rates, spectrum competition, and security [1]. FSOC is the best means to realize large-capacity and high-speed network [2]. Inter-satellite FSOC network has become a major development direction [3–6].

It is difficult to form a high-speed, real-time and high-throughput FSOC network with low SWaP value for traditional "point-to-point" FSOC [7,8]. Agile laser beams with fast steering and tracking will be required for FSOC network with low SWaP value. The cost and the complexity are other important issues. Modulated retro reflector (MRR) only needs Pointing, Acquisition and Tracking (PAT) at one end, and a corner reflector or a"cat's eye" onboarded at the other end [9,10]. MRR is usually a few kilograms, and its power consumption is a few watts [11], which meets the requirements of low SWaP value of micro satellites. At present, most of the research focuses on the application of MRR in point-to-point communication scenarios [12]. Using the MRR Array,"point-to-multipoints" laser communication can be realized. For example, the all-sky coverage inter-satellite omnidirectional optical communication (ISOC) based on MEMS modulation reflector is being developed by the Jet Propulsion Laboratory [13].

Due to the short insight time of inter-satellite laser communication, satellite networking requires relay satellites to increase the data transmission time and communication range. Two Way Relay Channel (TWRC) is a basic unit in FSOC network. In order to further improve the real-time performance and throughput of FSOC networks, this paper proposes an inter-satellite ANC scheme based on MRR (MRR ANC), which is used to meet the demand of real-time and high-throughput information sharing and exchange for FSOC network of micro satellites. MRR ANC system model is established, and the power allocation, system throughput and average BER of MRR ANC system are simulated and analyzed, and the feasibility of MRR ANC system is evaluated. The results show that MRR ANC system can improve the system throughput with low SWaP value. MRR ANC system rate and BER performances can be improved by using power allocation.

The remainder of this paper is organized as follows: Sect. 2 presents MRR ANC system design. Section 3 gives the system model for MRR ANC. Section 4 proposes optimal power allocation for MRR ANC. Section 5 calculates the throughput for MRR ANC. Section 6 presents our simulation analyses and discussion. Finally, Sect. 7 concludes this paper.

2 MRR ANC System Design

The communication process of traditional point-to-point FSOC in TWRC channel is shown in Fig. 1. To complete the optical relay communication, the system requires at least three PATs and four time slots for the TWRC information

exchange. Taking the PAT used on the NASA LLCD (Lunar Laser Communications Demonstration) [1] as an example, each terminal will require a weight resource of about 30.7 kg, power consumption of about 90 W, and volume of 315 mm × 261 mm × 185 mm. Due to the small divergence angle and precise pointing of the laser beam, PAT has certain requirements on the attitude and stability of the satellite platform.

MRR as FSOC terminal can realize "point-to-multipoints" communication, can save the PAT on the satellites, so it is suitable for inter-satellite FSOC of micro satellites. The working principle of MRR and the TWRC channel information exchange process are shown in Fig. 2 and Fig. 3.

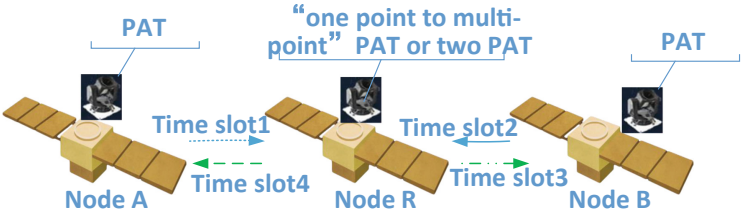

Fig. 1. Schematic diagram of traditional point-to-point laser communication terminal information exchange in TWRC

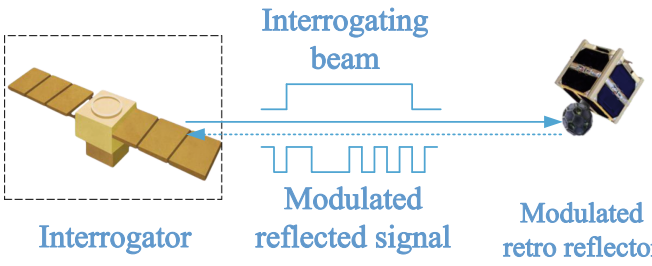

Fig. 2. MRR system architecture diagram

This paper proposes MRR ANC system as shown in the Fig. 4. The satellite FSOC network based on MRR takes the main satellite as the network node, the "one-point-to-multipoint" PAT is installed on the main satellite, and MRR array is installed on the sub-satellite. The main satellite is the interrogator and the sub-satellite is the passive end. The main satellite sends the interrogating beam to the sub-satellite, and the sub-satellite modulates the information on the interrogating beam to complete the inter-satellite bidirectional communication. The network structure can be rapidly and dynamically reconstructed to adapt

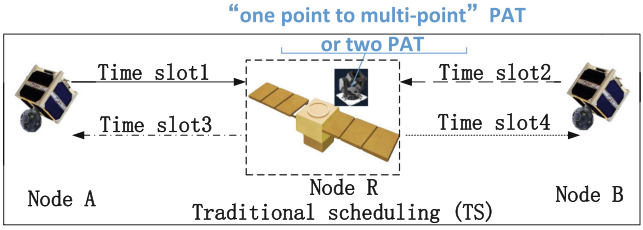

Fig. 3. Information exchange between MRR terminals on the help of relay

the rapidly changing space situation and mission. Compared with the ANC system implemented by the traditional FSOC terminal, the MRR ANC system can save the PATs on subsatellites. By using ANC, the packet exchange between two end nodes can be completed in two time slots with the help of relay node, and the throughput can be increased by two times theoretically.

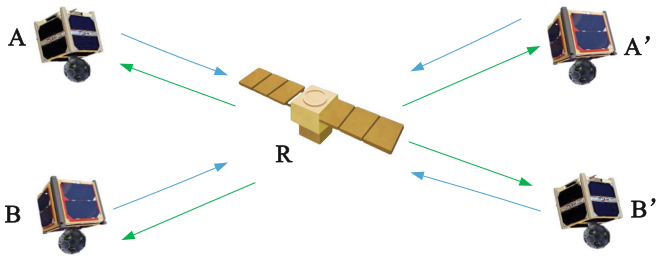

Fig. 4. MRR ANC system architecture diagram

Comparison of transmission time slots between ANC and traditional scheme is shown in the Fig. 5. The traditional scheduling needs 4 time slots to complete the information exchange between subsatellite A and B. The MRR ANC system can complete the information exchange in 2 time slots. This system can be used as the basic unit of FSOC network.

3 System Model

The transmission equation of conventional FSOC can be expressed as [14]

$$P_{\mathrm{STS}} = P_{\mathrm{Las}} G_{\mathrm{T}} L_{\mathrm{T}} L_{\mathrm{R}} T_{\mathrm{atm}} G_{\mathrm{rec}} L_{\mathrm{rec}} L_{PE}. \tag{1}$$

For a given modulation reflector antenna gain and modulation efficiency, the MRR transmission equation can be expressed as:

$$P_{\mathrm{SMRR}} = P_{\mathrm{Las}} G_{\mathrm{T}} L_{\mathrm{T}} L_{\mathrm{R}} T_{\mathrm{atm}} G_{\mathrm{MRR}} L_{\mathrm{MRR}} M L_{\mathrm{R}} T_{\mathrm{atm}} G_{\mathrm{rec}} L_{\mathrm{rec}} L_{PE}. \tag{2}$$

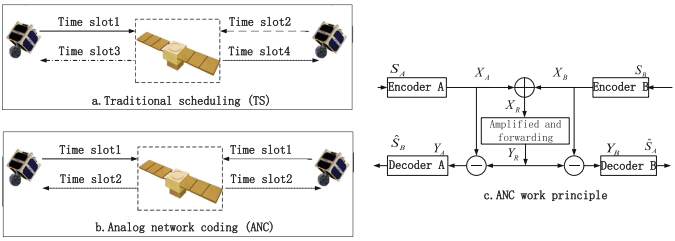

Fig. 5. MRR ANC work principle diagram

In Eqs. 1 and 2, P_{STS} denotes the optical signal received by the receiver, P_{SMRR} is the power of the MRR signal received by the main satellite, P_{Las} is the emitted power, G_T is the transmitter antenna gain at the interrogator, L_T is the transmitting antenna loss, L_R is the loss of free space, T_{atm} is the atmospheric transmission loss, G_{MRR} is the optical gain of the MRR, L_{MRR} is the optical loss of the MRR, M is the modulation coefficient of the MRR, G_{rec} is the optical antenna gain of the interrogator, L_{rec} is the optical loss of the receiver. Atmospheric losses are not considered because we tend to establish inter-satellite link.

The MRR antenna gain, optical loss, modulation efficiency are increased based on the transmitter and receiver related terms. Compared with the traditional laser communication link, the MRR link has higher distance loss, attenuates as $1/R^4$ not $1/R^2$. On-off Keying (OOK) modulation format and intensity modulation with direct detection (IM/DD) are used. The signal reception model can be expressed as $y = \eta hx+n$, where y is the received signal, η is the photoelectric conversion efficiency of the receiver, h represents channel state, $x \in \{0, 1\}$ denotes binary signal, n is white Gaussian noise.

For MRR ANC system, the two subsatellites A and B modulate signals on top of the interrogating beam and reflect back to the main satellite R simultaneously in the first time slot. The main satellite receives the imposed signals $y_{\mathrm{R}} = h_{\mathrm{A1}}\sqrt{P_{\mathrm{A}}}\,(X_{\mathrm{A}} + z_{\mathrm{RA}}) + h_{\mathrm{B1}}\sqrt{P_{\mathrm{B}}}\,(X_{\mathrm{B}} + z_{\mathrm{RB}}) + z_{\mathrm{R}}$, where P_A and P_B represent the power of the main satellite to subsatellites A and B, respectively. h_{A1} and h_{B1} are respectively the channel gain between A and R, B and R. z_{RA}, z_{RB} and z_{R} are Gaussian white noises with zero mean and σ_{n}^2 variance. h_{A1} and h_{B1} include channel attenuation from the interrogating beam emitted by the main satellite to the sub-satellite, channel attenuation from the signal light reflected by the sub-satellite, and random channel attenuation due to pointing error of the main satellite.

The main satellite R amplifies and forwards the received signal Y_R with the gain β in the second time slot. Assume that the channel state is known, the received signal of subsatellite A and B can be denoted by $y_{\mathrm{A}} = \beta h_{\mathrm{A2}} y_{\mathrm{R}} + z_{\mathrm{A}}$ and $y_{\mathrm{B}} = \beta h_{\mathrm{B2}} y_{\mathrm{R}} + z_{\mathrm{B}}$ respectively. z_{A} and z_{B} are Gaussian white noise with zero mean, the variance of σ_{n}^2. h_{A2} and h_{B2} include the inherent channel attenuation between the satellite and the main satellite and random channel attenuation due

to pointing error. Y_R is estimated based on Linear Minimum Mean Square Error (LMMSE), the amplification factor β can be expressed as [15].

$$\beta = \sqrt{P_{\mathrm{R}} \Big/ \left(\left|h_{\mathrm{A1}}\right|^2 P_{\mathrm{A}} + \left|h_{\mathrm{B1}}\right|^2 P_{\mathrm{B}} + \left(\left|h_{\mathrm{A1}}\right|^2 P_{\mathrm{A}} + \left|h_{\mathrm{B1}}\right|^2 P_{\mathrm{B}} + 1 \right) \sigma_{\mathrm{n}}^2 \right)}. \tag{3}$$

Assuming that the subsatellite A and B can accurately predict the channel state, the opposite signal can be obtained by subtracting its own signal from the received signals. The opposite signal can be denoted as $y'_{\mathrm{A}} = \beta\sqrt{P_{\mathrm{B}}} h_{\mathrm{A2}} h_{\mathrm{B1}} X_{\mathrm{B}} + \beta h_{\mathrm{A2}} z_{\mathrm{R}} + z'_{\mathrm{A}}$, $y'_{\mathrm{B}} = \beta\sqrt{P_{\mathrm{A}}} h_{\mathrm{A1}} h_{\mathrm{B2}} X_{\mathrm{A}} + \beta h_{\mathrm{B2}} z_{\mathrm{R}} + z'_{\mathrm{B}}$, where z'_{A} and z'_{B} are sum of $\left|h_{\mathrm{A1}}\right|^2 P_{\mathrm{A}} \sigma_{\mathrm{n}}^2$ and σ_{n}^2, sum of $\left|h_{\mathrm{B1}}\right|^2 P_{\mathrm{B}} \sigma_{\mathrm{n}}^2$ and σ_{n}^2 respectively. The signal-to-noise ratio of the signals received by subsatellites A and B can be expressed as [16,17]:

$$\gamma_{\mathrm{A}} = \beta^2 \left|h_{\mathrm{A2}}\right|^2 \left|h_{\mathrm{B1}}\right|^2 P_{\mathrm{B}} \Big/ \left(\left(\beta^2 \left|h_{\mathrm{A2}}\right|^2 + \left|h_{\mathrm{A1}}\right|^2 P_{\mathrm{A}} + 1 \right) \sigma_{\mathrm{n}}^2 \right). \tag{4}$$

$$\gamma_{\mathrm{B}} = \beta^2 \left|h_{\mathrm{A1}}\right|^2 \left|h_{\mathrm{B2}}\right|^2 P_{\mathrm{A}} \Big/ \left(\left(\beta^2 \left|h_{\mathrm{B2}}\right|^2 + \left|h_{\mathrm{B1}}\right|^2 P_{\mathrm{B}} + 1 \right) \sigma_{\mathrm{n}}^2 \right). \tag{5}$$

The achieved rate of half duplex TWRC system using MRR ANC based on γ_{A} and γ_{B} is [16,17]

$$\begin{aligned} R_{\mathrm{sum}} &= \tfrac{1}{2} \log\left(1 + \gamma_{\mathrm{A}}\right) + \tfrac{1}{2} \log\left(1 + \gamma_{\mathrm{B}}\right) \\ &= \tfrac{1}{2} \log\left(1 + \gamma_{\mathrm{A}}\right)\left(1 + \gamma_{\mathrm{B}}\right) \end{aligned} \tag{6}$$

4 Optimal Power Allocation

In MRR ANC system, in order to minimize the outage probability and maximize the total amount of system information exchange, power allocation is needed. The goal of power allocation can be to achieve the maximum system rate, the minimum outage probability, the best signal-to-noise ratio or the best bit error rate. In this paper, the optimal power allocation target is to maximize sum rate of MRR ANC system in TWRC channel.

The problem can be equivalent to maximizing the sum rate on the constraint of $P_{\mathrm{A}} + P_{\mathrm{B}} + P_{\mathrm{R}} = P_{\mathrm{T}}$:

$$\left(P_{\mathrm{A}} P_{\mathrm{B}} P_R\right) = \max_{P_{\mathrm{A}} P_{\mathrm{B}} P_{\mathrm{R}}} R_{\mathrm{sum}}\left(R\right) P_{\mathrm{A}} + P_{\mathrm{B}} + P_{\mathrm{R}} = P_{\mathrm{T}} \tag{7}$$

According to Eq. 6, Eq. 7 is equivalent to

$$\left(P_{\mathrm{A}} P_{\mathrm{B}} P_R\right) = \max_{P_{\mathrm{A}} P_{\mathrm{B}} P_{\mathrm{R}}} \left(1 + \gamma_{\mathrm{A}}\right)\left(1 + \gamma_{\mathrm{B}}\right) P_{\mathrm{A}} + P_{\mathrm{B}} + P_{\mathrm{R}} = P_{\mathrm{T}} \tag{8}$$

Since $\left(1 + \gamma_{\mathrm{A}}\right)\left(1 + \gamma_{\mathrm{B}}\right) = 1 + \gamma_{\mathrm{A}} + \gamma_{\mathrm{B}} + \gamma_{\mathrm{A}}\gamma_{\mathrm{B}} \leq \left(1 + \left(\gamma_{\mathrm{A}} + \gamma_{\mathrm{B}}\right)/2\right)^2$, only when $\gamma_{\mathrm{A}} = \gamma_{\mathrm{B}}$, $\left(1 + \gamma_{\mathrm{A}}\right)\left(1 + \gamma_{\mathrm{B}}\right)$ can reach the upper limit, and if $\gamma_{\mathrm{A}} + \gamma_{\mathrm{B}}$ achieves the maximum value, the upper limit will reache the maximum. Because $\frac{1}{\gamma_{\mathrm{A}}} + \frac{1}{\gamma_{\mathrm{B}}} = \frac{\gamma_{\mathrm{A}} + \gamma_{\mathrm{B}}}{\gamma_{\mathrm{A}}\gamma_{\mathrm{B}}} \geq \frac{4}{\gamma_{\mathrm{A}} + \gamma_{\mathrm{B}}}$, if and only if $\gamma_{\mathrm{A}} = \gamma_{\mathrm{B}}$, $\frac{1}{\gamma_{\mathrm{A}}} + \frac{1}{\gamma_{\mathrm{B}}}$ reaches the lower

limit and if $\gamma_A + \gamma_B$ achieves the maximum, the lower limit will be minimum. Hence, if $\frac{1}{\gamma_A} + \frac{1}{\gamma_B}$ reaches the lower limit, $(1+\gamma_A)(1+\gamma_B)$ will be the maximum. By substituting Eqs. 4 and 5, we will get

$$\frac{1}{\gamma_A} + \frac{1}{\gamma_B} = \frac{\left(\left(\beta^2 |h_{A2}|^2 + |h_{A1}|^2 P_A + 1\right)\sigma_n^2\right)}{\beta^2 |h_{A2}|^2 |h_{B1}|^2 P_B} + \frac{\left(\left(\beta^2 |h_{B2}|^2 + |h_{B1}|^2 P_B + 1\right)\sigma_n^2\right)}{\beta^2 |h_{A1}|^2 |h_{B2}|^2 P_A} \tag{9}$$

Substituting Eq. 3 into Eq. 9, we will get

$$\frac{1}{\gamma_A} + \frac{1}{\gamma_B} = \frac{P_R |h_{A2}|^2 \sigma_n^2 + (P_A |h_{A1}|^2 \sigma_n^2 + \sigma_n^2)[P_A |h_{A1}|^2 + P_B |h_{B1}|^2 + (P_A |h_{A1}|^2 + P_B |h_{B1}|^2 + 1)\sigma_n^2]}{|h_{A2}|^2 |h_{B1}|^2 P_R P_B} + \frac{P_R |h_{B2}|^2 \sigma_n^2 + (P_B |h_{B1}|^2 \sigma_n^2 + \sigma_n^2)[P_A |h_{A1}|^2 + P_B |h_{B1}|^2 + (P_A |h_{A1}|^2 + P_B |h_{B1}|^2 + 1)\sigma_n^2]}{|h_{A1}|^2 |h_{B2}|^2 P_A P_R} \tag{10}$$

Using Lagrangian least multiplier method to find the minimum value of Eq. 10 on the constrains of $P_A + P_B + P_R = P_T$, the optimal power allocation can be obtained. In order to simplify the problem, it is assumed that the power of the continuous optical signal transmitted by the relay node is large enough and the Gaussian white noise carried by the continuous optical signal is ignored [18]. Consider power allocation of the power reflected back by MRR and the power of the relay node (P_{MRRA}, P_{MRRB}, P_R), on the constraint of $P_{MRRA} + P_{MRRB} + P_R = P'_T$. The channel attenuation coefficients of the signals reflected from the sub satellite MRR of A and B are the same as that of h_{A2} and h_{B2}. Formula 10 can be simplified as

$$\frac{1}{\gamma_A} + \frac{1}{\gamma_B} = \frac{\left(|h_{A2}|^2 P'_T \sigma_n^2 + \sigma_n^4\right) P_{MRRA} + \left(|h_{B2}|^2 P'_T \sigma_n^2 + \sigma_n^4\right) P_{MRRB}}{|h_{A2}|^2 |h_{B2}|^2 P_{MRRA} P_{MRRB} P_R} \tag{11}$$

Using Lagrange multiplier method, the optimal power allocation can be obtained as follows [15]

$$P_R = \frac{1}{2} P'_T \tag{12}$$

$$P_{MRRA} = \frac{1}{2 + 2\sqrt{\frac{|h_{A2}|^2 P'_T \sigma_n^2 + \sigma_n^4}{|h_{B2}|^2 P'_T \sigma_n^2 + \sigma_n^4}}} P'_T \tag{13}$$

$$P_{MRRB} = \frac{1}{2 + 2\sqrt{\frac{|h_{B2}|^2 P'_T \sigma_n^2 + 1\sigma_n^4}{|h_{A2}|^2 P'_T \sigma_n^2 + 1\sigma_n^4}}} P'_T \tag{14}$$

5 Throughput

The upper and lower limits of channel capacity can be calculated. The throughput is compared by calculating the upper bound of traditional scheduling method and the lower bound of channel capacity of MRR ANC system. Suppose that

the channels between A and R, B and R are independent and obey Gaussian white noise distribution, and all nodes have the same transmit power. According to [19], the theoretical upper limit of channel capacity of traditional scheduling method is

$$C_{\text{traditional}} = \alpha \left(\log\left(1+2R_{\text{SN}}\right) + \log\left(1+R_{\text{SN}}\right)\right) \tag{15}$$

The theoretical lower limit of the channel capacity of the ANC system is

$$C_{\text{ANC}} = 4\alpha \log\left(1+\frac{R_{\text{SN}}^2}{3R_{SN}+1}\right) \tag{16}$$

6 Simulation Results Analysis and Discussion

In this section, we perform numerical simulation on sum rage, BER and capacity of MRR ANC. It is assumed that the positional relationship between the relay node and the nodes at both ends is a straight line, and the relay node is located between the two end nodes. See Table 1 for the parameters used.

Performance of optimal power allocation and the unified power allocation (the reflected power of the two endpoints and the transmission power of the relay node are the same, respectively are 1/3 of the total power) are compared with the achievable sum rates, BER and capacity.

Table 1. Parameters for simulations

Term	Parameter	Formula	Value
Tx power	≤ 5 W	Measured	37 dBm
Transmitter loss	–	Measured	−1.0 dB
Tx antenna gain	Full angle e^{-2} divergence	$32/\theta_{div}, \theta_{div} = 30\mu rad$	105.5 dB
Interrogator range loss	$R = 200$ km, $\lambda = 850$ nm	$(\lambda/4\pi R)^2$	−294.4 dB
Electro-optic modulator	Insert loss	measured	−4 dB
MRR T/R Antenna gain	$D_{retro} = 5$ cm, $S = 0.4$	$(\pi D_{retro}/\lambda)^4 S$	213.8 dB
Range loss(retro return)	$R = 200$ km, $\lambda = 850$ nm	$(\lambda/4\pi R)^2$	−249.4 dB
Receiver antenna gain	$D_{rec} = 20$ cm	$(\pi D_{rec}/\lambda)^2$	117.4 dB
Receiver loss	Fiber coupling loss	–	−1 dB
Receiver sensitivity	S_v	$(BER = 10^{-10})$	−38 dB
Predicted receiver power	–	–	−35 dB
Noise standard deviation	σ_{n}	–	$10^{-7}\text{A}/\sqrt{Hz}$
Pointing error loss	L_{PE}	–	−1 dB

Regardless of whether the distances between the nodes A and B and the relay node are the same or different, the sum rate that can be achieved by the optimal power allocation scheme is better than the unified power allocation scheme as shown in Fig. 6 and Fig. 7. When the distance between the end node and the relay node is the same, the achievable rate is higher. When the distance between the end node and the relay node is different, the sum rate achieved

by the Lagrange multiplier power allocation scheme is more different than the unified power allocation scheme.

When the two end nodes A and B are at the same distance from the relay node, the BER performance of the end nodes is compared. Figure 8 shows that the BER performance that can be achieved by the optimal power allocation scheme is better than that of the unified power allocation scheme.

Figure 9 and Fig. 10 shows that, with the increase of the signal-to-noise ratio, the throughput of ANC are both 1.81 times of the traditional scheduling (the signal-to-noise ratio of 65 dB), no matter ignoring the noise carried by the interrogating beam or considering the noise. The result is consistent with the theoretical derivation of [19]. It can be proved that the simplified method of power allocation in this paper is reasonable.

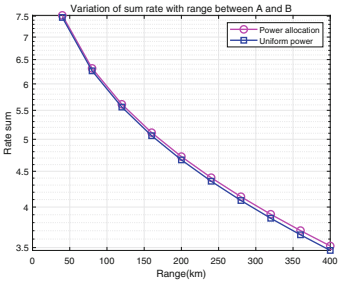

Fig. 6. The distance from node A or B to relay node is the same

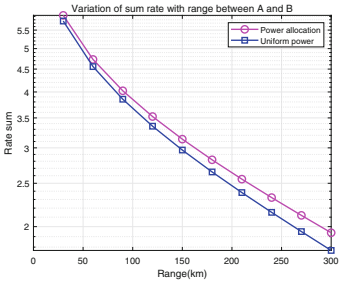

Fig. 7. The distance from node A or B to relay node is different

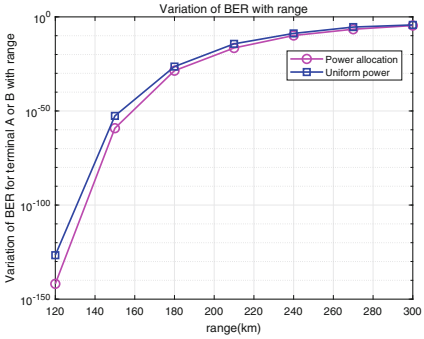

Fig. 8. Variation of BER with distance in MRR ANC systems

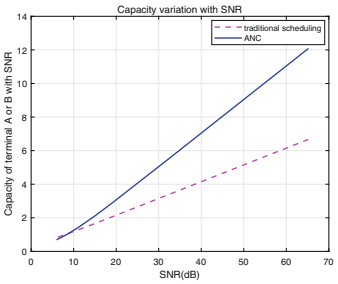

Fig. 9. Capacity bounds as functions of SNR, ignoring noise of interrogating laser

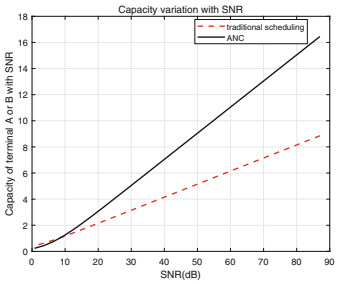

Fig. 10. Capacity bounds as functions of SNR, considering noise of interrogating laser

7 Conclusion

In this paper, an MRR ANC system is designed in TWRC to meet the needs of real-time, high throughput data exchange and low SWaP value of micro-satellite space FSOC network. The model of MRR ANC system is established. In order to achieve the best quality of communication service, the power allocation scheme of MRR ANC system is proposed with the goal of maximum sum rate.

We believe that MRR ANC's low SWaP value, suitable for small satellite platforms, and "point to point" characteristics will make small satellite inter-satellite laser communication network a reality. The limitations of MRR ANC lies in its communication distance. The difficulty with ANC implementation is to improve the performance of the modulated reflector under low SWaP conditions.

Simulation results show that the sum rate of the system is better than that of the unified power allocation scheme after the optimal power allocation, and the BER performance of the power allocation scheme with the target of maximum sum rate is also better than that of the unified power allocation scheme under the same communication distance. By comparing the communication capacity of MRR ANC with that of traditional scheduling, it can be concluded that the throughput of MRR ANC is 1.8 times of that of traditional scheduling when the signal-to-noise ratio is 65 dB. The simulation results show that MRR ANC system is feasible, which provides a new method for small satellite laser communication network.

In the future, we can further consider the research of power allocation with the minimum outage probability and the best bit error rate performance as the optimization objectives. At the same time, the optimization scheme of power allocation can also be applied to physical layer network coding (PNC).

References

1. Boroson, D.M., Robinson, B.S.: The lunar laser communication demonstration: NASA's first step toward very high data rate support of science and exploration missions. In: Elphic, R.C., Russell, C.T. (eds.) The Lunar Atmosphere and Dust Environment Explorer Mission (LADEE), pp. 115–128. Springer, Cham (2015). https://doi.org/10.1007/978-3-319-18717-4_6
2. Chang, C.W., Cheng, L.Y., Luo, D., et al.: Progress of space laser communication and conception of its application in space based networks. J. Spacecr. TT C Technol. **34**(2), 176–183 (2015)
3. Pulliam, J., et al.: TSAT network architecture. In: MILCOM 2008–2008 IEEE Military Communications Conference, pp. 115–128. IEEE (2008). https://doi.org/10.1109/MILCOM.2008.4753508
4. Thomas, S., Andreas, H., et al.: ESA long-term monitoring of space debris in GEO, GTO and first surveys of MEO. In: 28th Inter-Agency Debris Coordination Committee (IADC) Meeting, International Association of Drilling Contractors IADC (2010)
5. Gao, D.R., Li, T.L., Sun, Y., et al.: Latest developments and trends of space laser communication. Chin. Opt. **11**(6), 901–913 (2018)
6. Jiang, H.L., Fu, Q., Zhao, Y.W., et al.: Development status and trend of space information network and laser communication. Chin. J. Internet Things **3**(2), 1–8 (2019)
7. Shubert, P., Cline, A., McNally, J., Pierson, R.: Design of low SWaP optical terminals for free space optical communications. In: Free-Space Laser Communication and Atmospheric Propagation XXIX, vol. 10096 (2017)
8. Radhakrishnan, R., Edmonson, W.W.: Survey of inter-satellite communication for small satellite systems: physical layer to network layer view. IEEE Commun. Surv. Tutor. **18**(4), 2442–2473 (2016)
9. Arnon, S., Barry, J., Karagiannidis, G., et al.: Advanced optical wireless communication systems. Hybrid RF/FSO Commun. (11), 273–302 (2012)
10. Li, X.: Research on the performance of the Modulating Retro-reflector free Space Optical Communications over Atmospheric Turbulence. Jilin Province (2020)
11. Goetz, P.G., et al.: Modulating retro-reflector lasercom systems for small unmanned vehicles. IEEE J. Sel. Areas Commun. **30**(5), 986–992 (2012)
12. Hu, J., Wang, J., Wang, K., et al.: The research on aperture averaging of modulating retro-reflector optical communication. In: 2020 International Conference on Wireless Communications and Signal Processing (WCSP) (2020)
13. Velazco, J.E., Griffin, J., Wernicke, D., et al.: High data rate inter-satellite omnidirectional optical communicator. In: 2019 IEEE Aerospace Conference (2019)
14. Liu, D.X., Zeng, J., Sun, S.F., et al.: Performance budget of space optical communication in atmospheric channel. Radio Commun. **536**(10), 68–72 (2020)
15. Xu, K., Zhang, D., Xu, Y., Ma, W.: On the equivalence of two optimal power-allocation schemes for A-TWRC. IEEE Trans. Veh. Technol. **63**(4), 1970–1976 (2014)
16. Rankov, B., Wittneben, A.: Spectral efficient protocols for halfduplex fading relay channels. IEEE J. Sel. Areas Commun. **25**(2), 379–389 (2007)
17. Katti, S.R.: Network Coded Wireless Architecture. Massachusetts Institute of Technology (2009)

18. Li, X., Zhao, X., Zhang, P., et al.: Probability density function of turbulence fading in MRR free space optical link and its applications in MRR free space optical communications. IET Commun. **11**(16), 2476–2481 (2017)
19. Katti, S., Gollakota, S., Katabi, D.: Embracing wireless interference: analog network coding. ACM SIGCOMM Comput. Commun. Rev. **9**(4), 1–14 (2007)